Supplementary Material

Construction of Molybdenum Vanadium Oxide/Nitride Hybrid Nanoplate Arrays for Aqueous Zinc-Ion Batteries and Reliable Insights into Reaction Mechanism

Yaxuan Zhuang,[a,1] Yulan Xie,[a,1] Ban Fei,[a] Daoping Cai,[a,*] Yaguang Wang,[a] Qidi Chen,[a] and Hongbing Zhan[a,*]

[a] College of Materials Science and Engineering, Fuzhou University, Fujian 350108, China.

Corresponding authors: Daoping Cai and Hongbing Zhan.

E-mail addresses: dpcai@fzu.edu.cn; hbzhan@fzu.edu.cn.

[1] These authors contribute equally to this work.

Experimental Section

Materials synthesis

Synthesis of MVOH NPAs: First, 1.5 g NH_4VO_3 and 2.9 g $H_2C_2O_4$ were dissolved in 50 mL deionized water under ultrasonication for 90 min and then formed a blue solution. Second, 0.22 g hexamethylene tetramine, 0.45 g $(NH_4)_6Mo_7O_{24}\cdot4H_2O$ and a piece of cleaned carbon cloth (2×3 cm, was pretreated by ethanol and deionized water separately with sonication for 10 min) were added into the above solution and kept at room-temperature for about 30 min. After that, the mixture was transferred into Teflon-lined autoclave and heated at 150 °C for 8 h. Finally, the CC@MVOH NPAs was rinsed with deionized water several times and dried at 70 °C for 12 h.

Synthesis of MVN NPAs: Typically, a piece of CC@MVOH NPAs and 3.0 g of melamine powder were put into horizontal quartz tube furnace, in which the melamine was placed at the upstream side. Then, the furnace was heated to 750 °C at 5 °C min^{-1} and maintained for 2 h in the mixing gas (95% Ar, 5% H_2). After cooling naturally, the CC@MVN was obtained. Similarly, the CC@VN was also synthesized without the addition of $(NH_4)_6Mo_7O_{24}\cdot4H_2O$. The mass loading of MVN NPAs was about 4.0 mg cm^{-2}, while the mass loading of VN was only about 0.8 mg cm^{-2}.

Materials characterization: The morphology, microstructure and composition of samples were investigated by high-resolution transmission electron microscope (HRTEM; Tecnai G2F20 S-TWIN), field emission scanning electron microscope (FESEM, Zeiss Supra55, Germany), X-ray diffractometer (XRD; D/maxUItimaIII Rigaku, Cu Kα radiation), X-ray photoelectron spectroscopy (XPS, Thermo Fisher Scientific, ESCALAB 250).

Electrochemical measurements: The Cyclic voltammetry (CV) curves, galvanostatic charge and discharge (GCD) tests and EIS analysis were performed by a electrochemical workstation (CHI 760E) at room temperature, and galvanostatic cycling tests were performed within the voltage window of 0.2–1.6 V on battery-testing instrument (LAND CT2001A). The electrochemical studies of the aqueous CC@*a*-MVO/MVN//Zn battery were measured by a two-electrode system. The

cathodes were prepared by cutting CC@a-MVO/MVN into a square (1×1 cm) and metallic Zn foil with the same area acts as anode, 3 M $ZnSO_4$ was employed as the electrolyte. The soft-packaged batteries were assembled by sandwiching separator and electrolyte between the CC@a-MVO/MVN cathode and Zn plate anode, then sealed by Al-plastic films. Both the CC@a-MVO/MVN and Zn plate were cut into 3 × 3 cm pieces. The thickness of Zn foil is about 0.5 mm and the dosages of electrolyte is 1 mL.
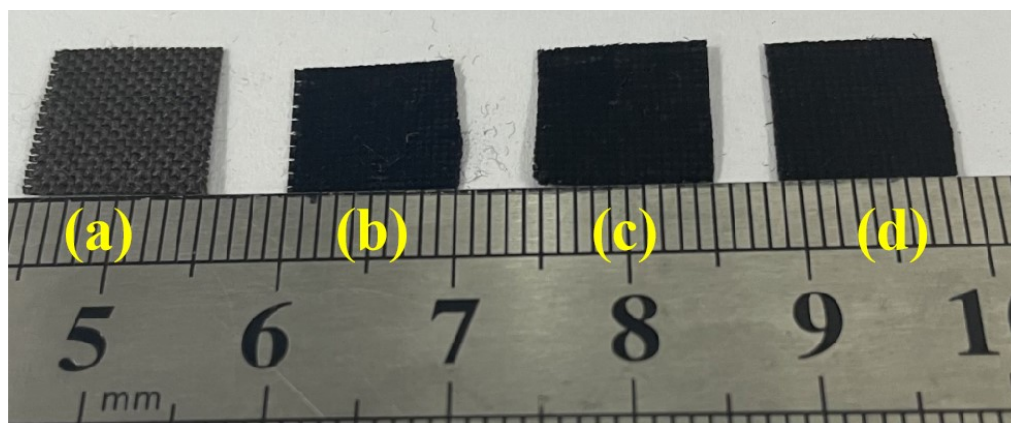
Figure S1. The photos of the (a) CC, (b) CC@MVOH NPAs, (c) CC@MVN NPAs, (d) CC@*a*-MVO/MVN HNPAs .
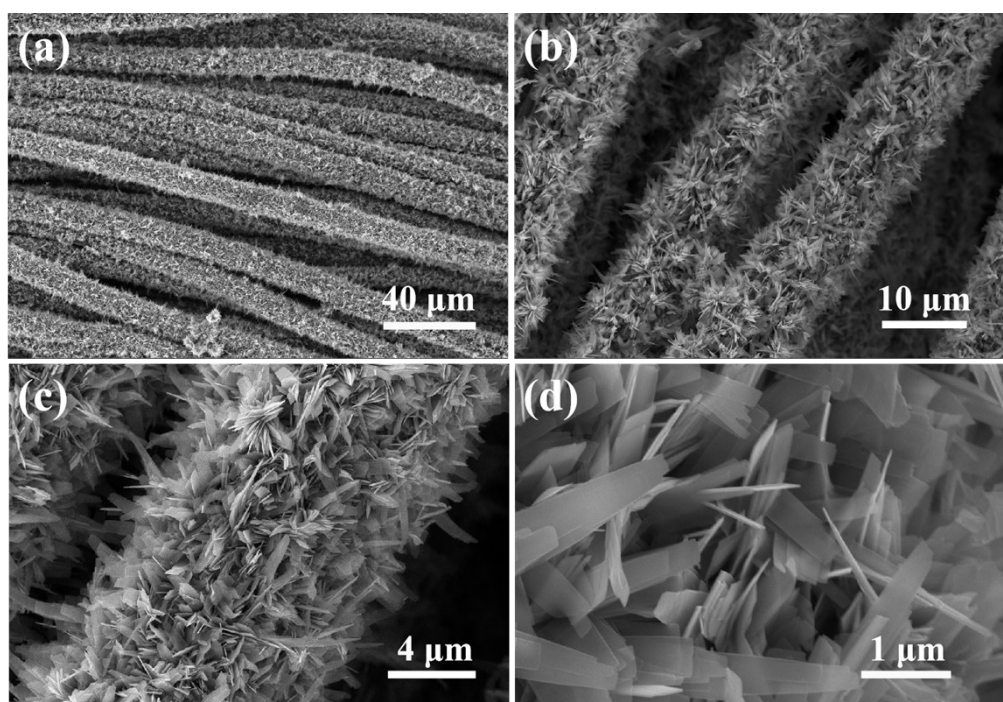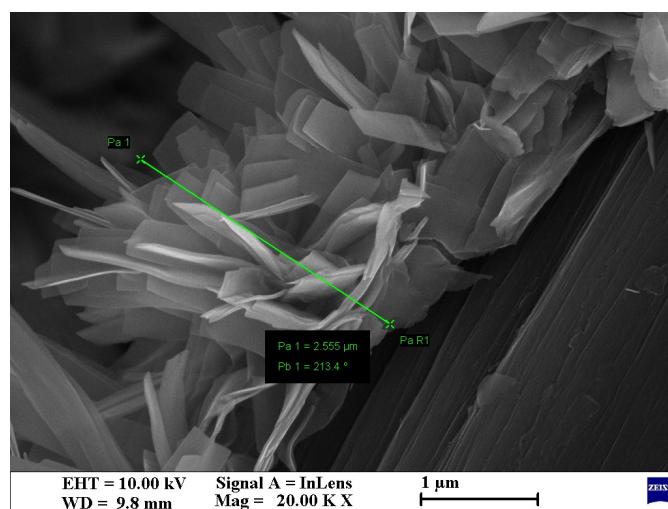

Figure S2. SEM images of the CC@MVOH NPAs.

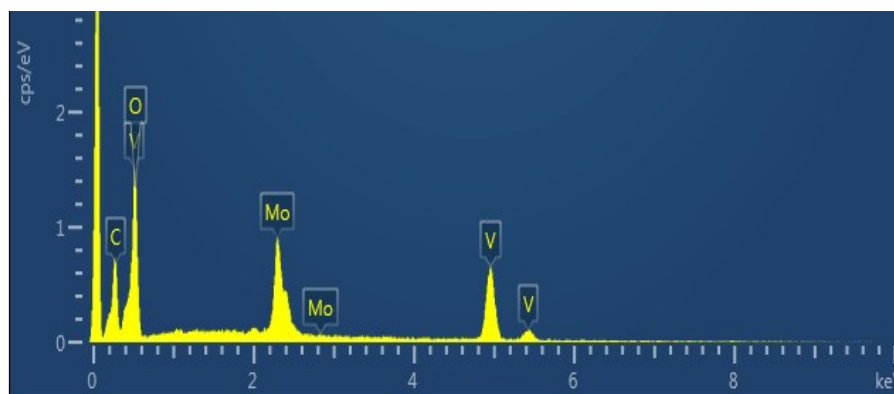**Figure S3.** Cross-section SEM image of the CC@MVOH NPAs.

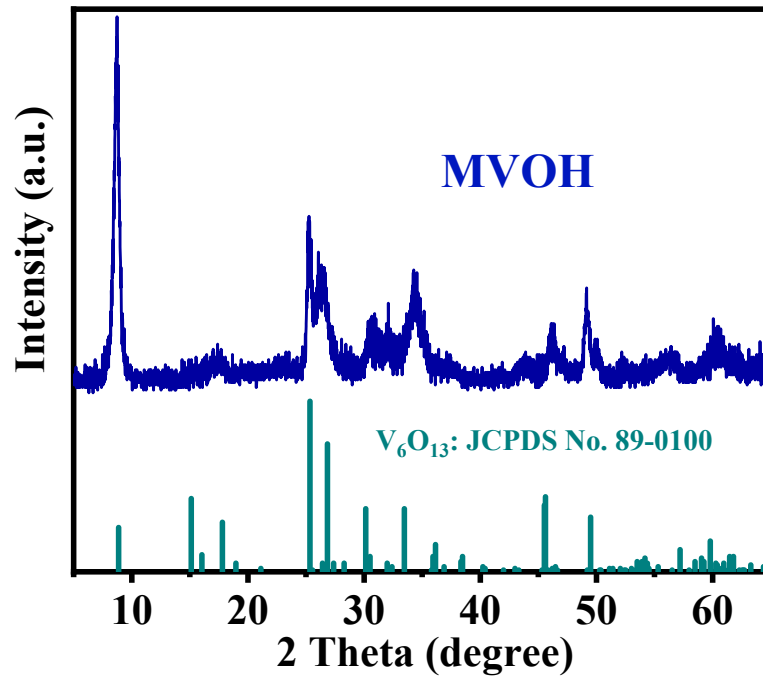
Figure S4. EDX spectrum of the CC@MVOH NPAs.

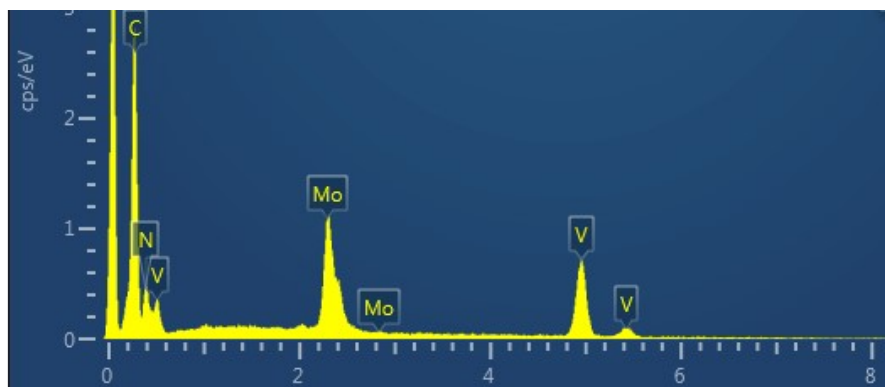**Figure S5.** XRD pattern of the MVOH NPAs.

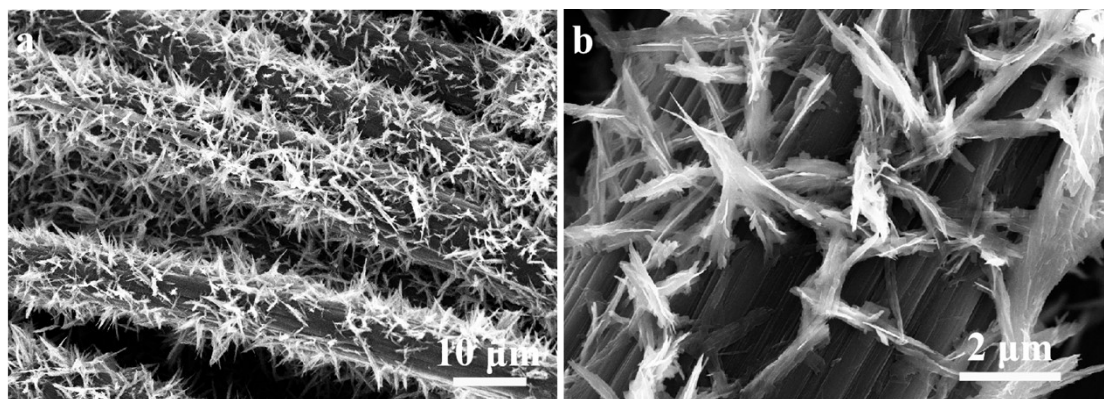**Figure S6.** EDX spectrum of the CC@MVN NPAs.
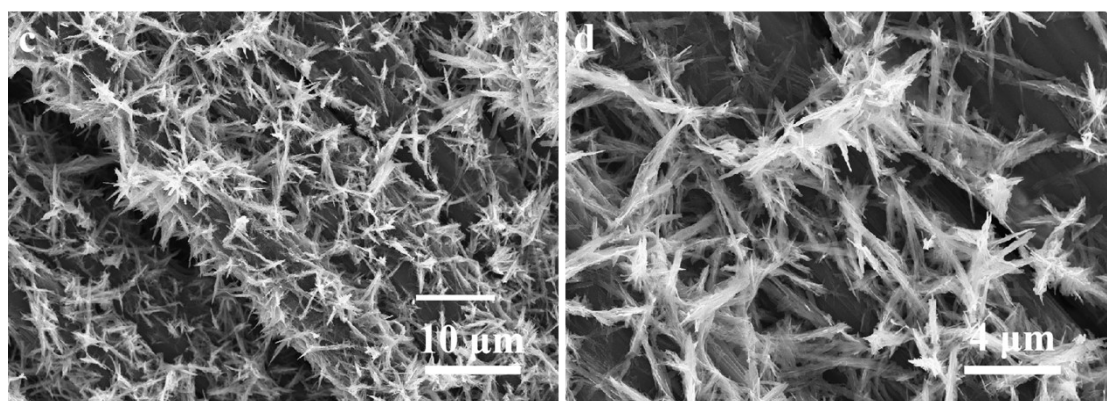
Figure S7. SEM images of the CC@VOH.

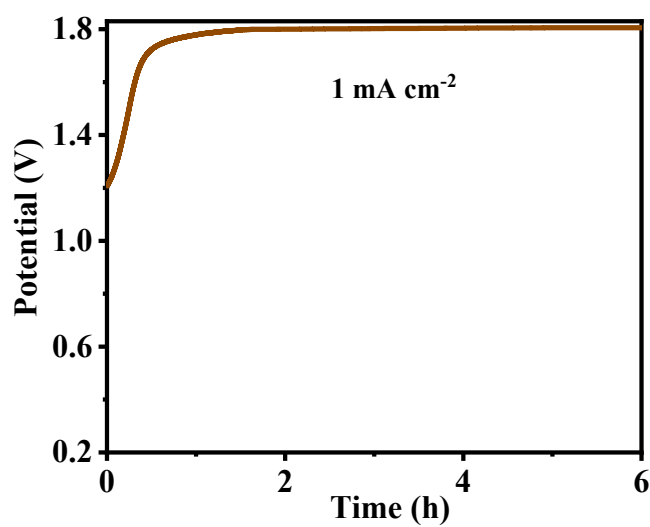**Figure S8.** SEM images of the CC@VN.

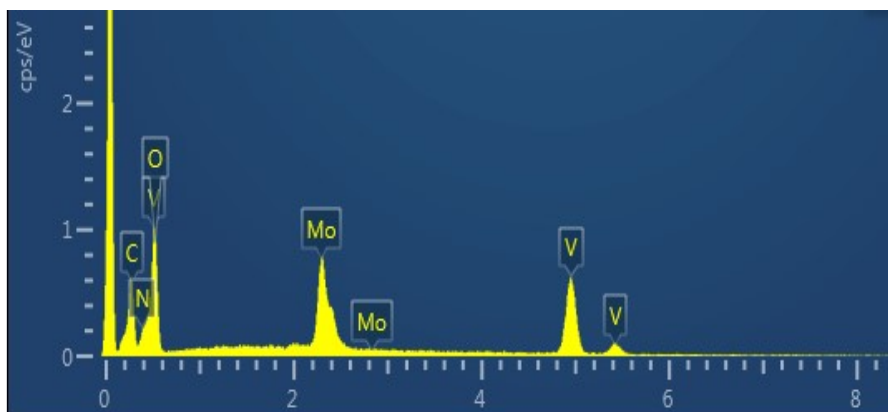**Figure S9.** The initial charging curve of the CC@MVN at 1.8 V for 6 h.

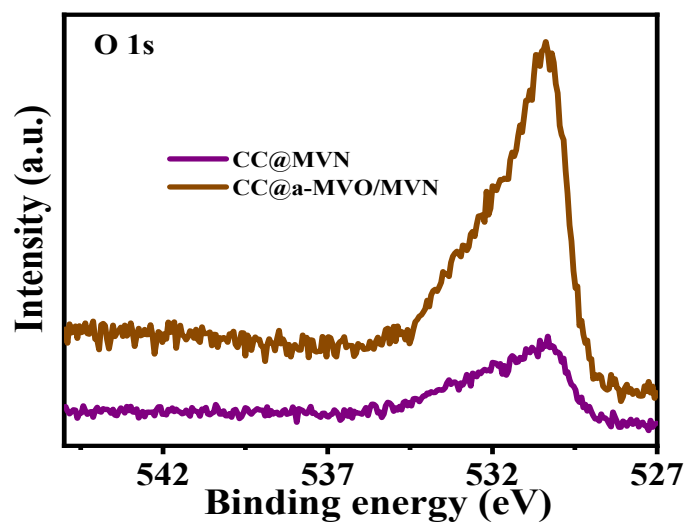**Figure S10.** EDX spectrum of the CC@*a*-MVO/MVN.

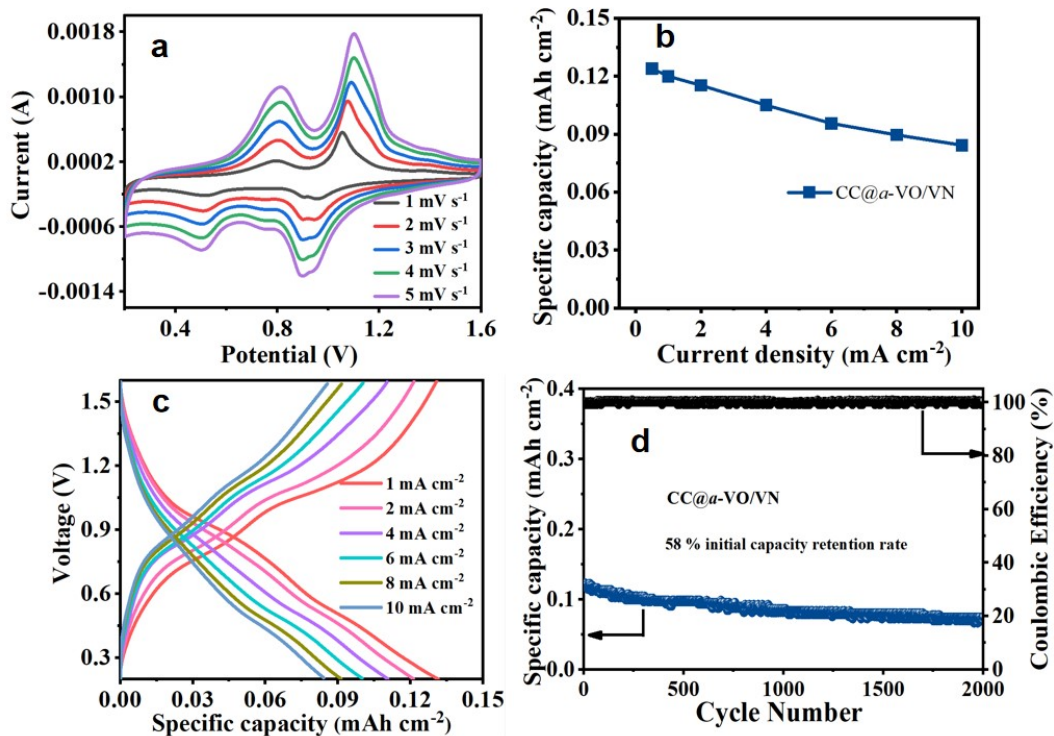**Figure S11.** O 1s spectra of the CC@MVN and CC@*a*-MVO/MVN.

Figure S12. (a) CV curves, (b) Rate performance, (c) GCD curves at different current densities and (d) Long-term cycling performance at 6 mA cm^{-2} of the CC@*a*-VO/VN//Zn battery.
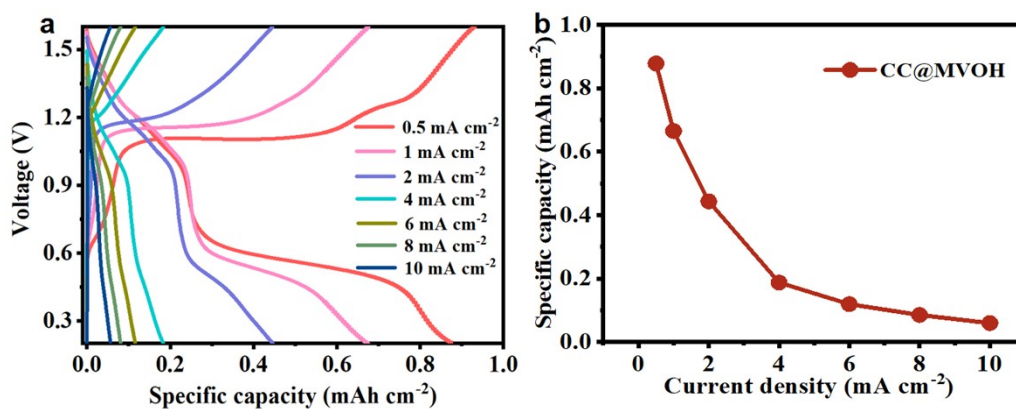

Figure S13. (a) GCD curves at different current densities and (b) Rate performance of the CC@MVOH//Zn battery.
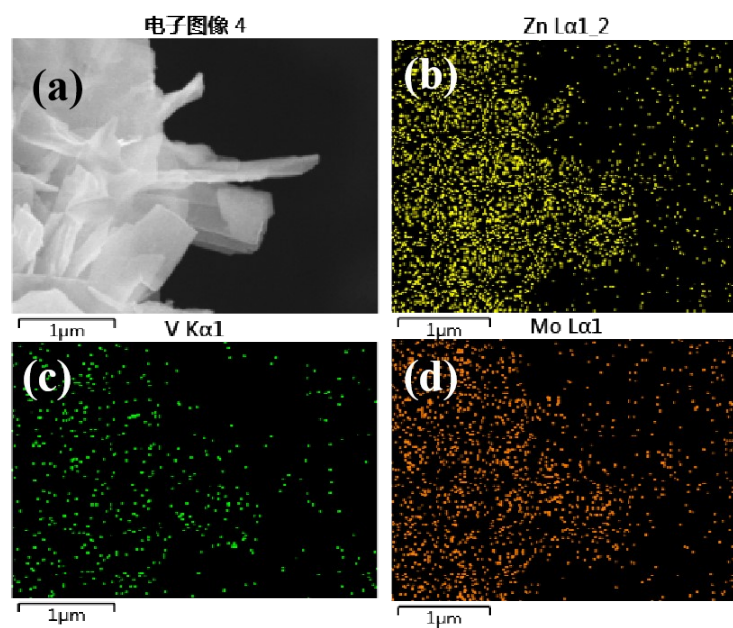
Figure S14. EDX mapping of the CC@*a*-MVO/MVN cathode at full discharge.
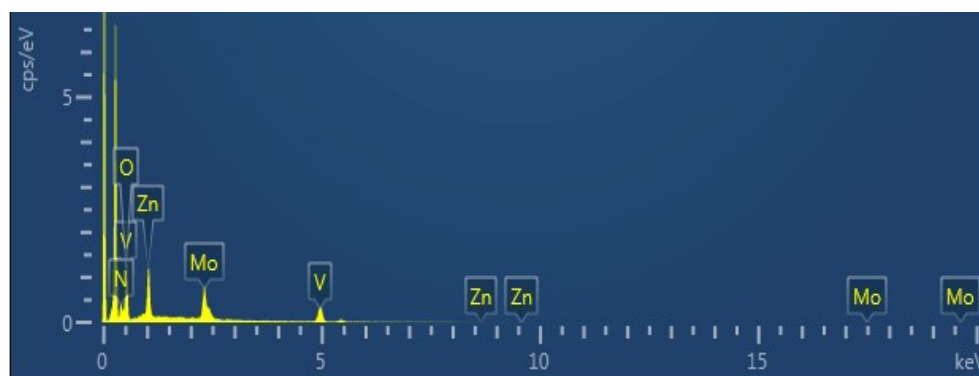
Figure S15. EDX spectrum of the CC@*a*-MVO/MVN cathode at full discharge.
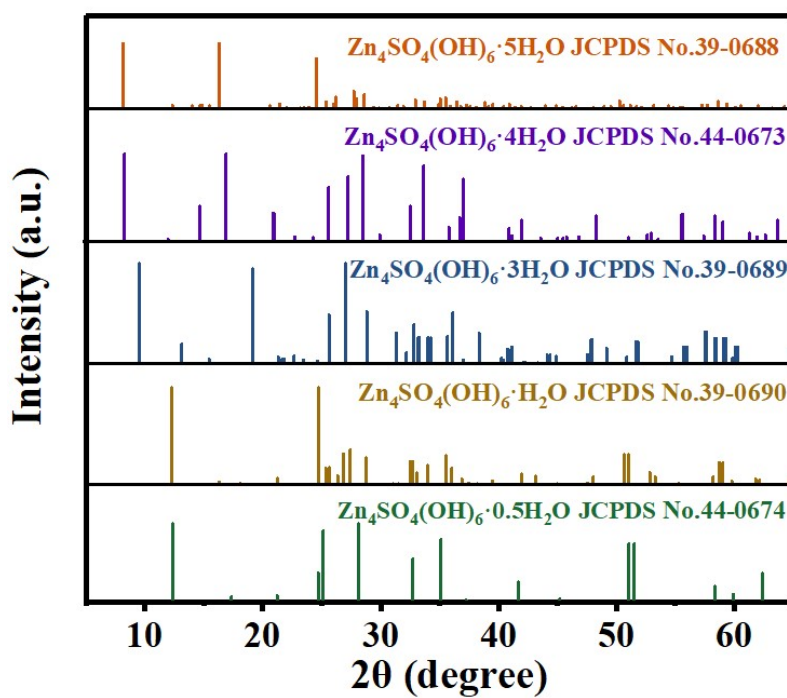
Figure S16. XRD patterns the $Zn_4(OH)_6SO_4 \cdot xH_2O$ byproduct at different dehydration degree.
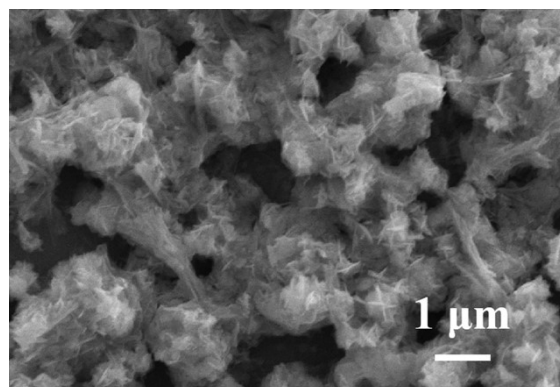
Figure S17. SEM image of the precipitate formed by mixing 1 M NaOH, 3 M $ZnSO_4$, and 1 M NH_4VO_3 solution drying at 70 ℃.
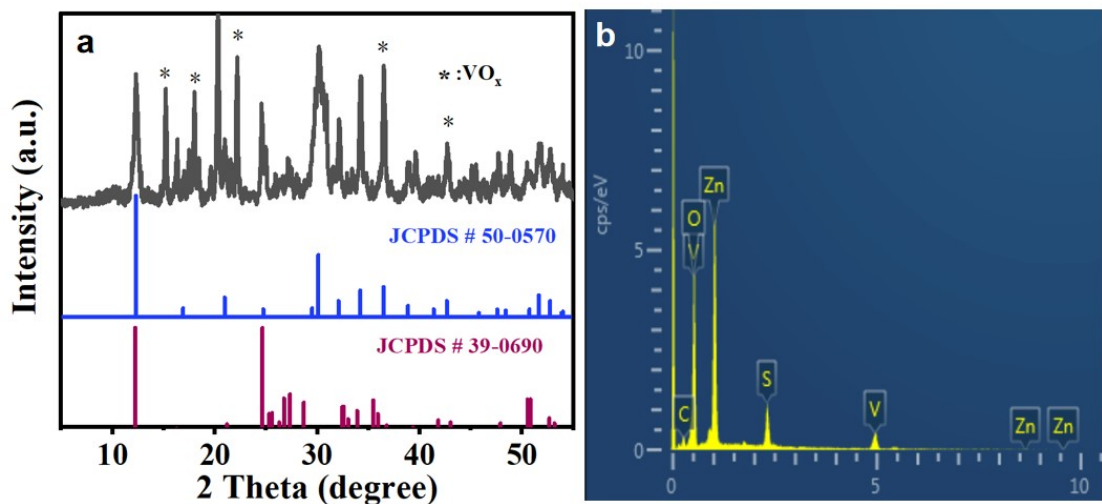
Figure S18. (a) XRD pattern and (b) EDX spectrum of the precipitate obtained by adding 1 M NaOH into 3 M $ZnSO_4$ and 1 M NH_4VO_3 solution and drying at 70 ℃.
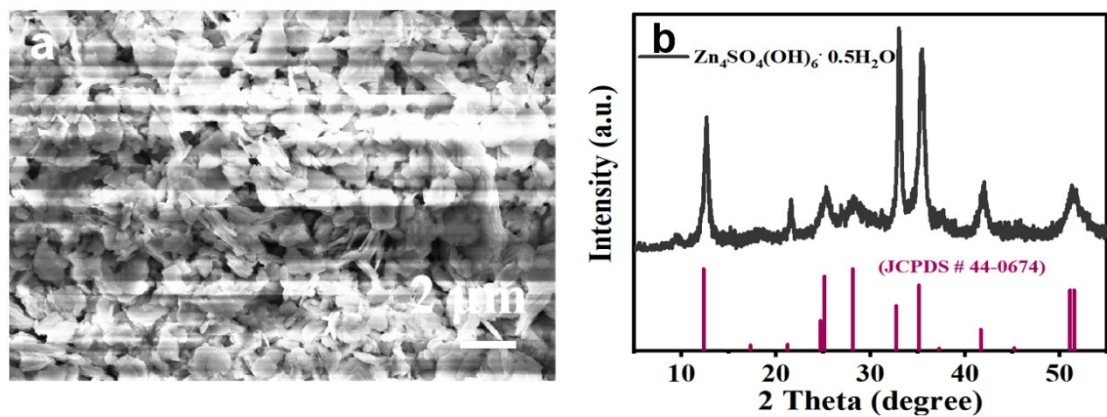
Figure S19. (a) SEM image and (b) XRD pattern of the precipitate obtained by adding 1 M NaOH into 3 M $ZnSO_4$ solution and dried at 130 ℃.
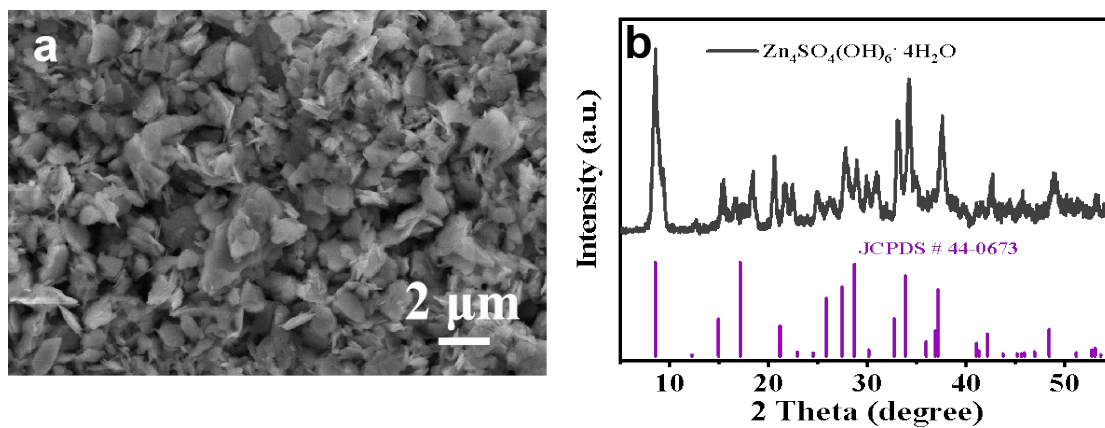
Figure S20. (a) SEM image and (b) XRD pattern of the precipitate obtained by adding 1 M NaOH into 3 M $ZnSO_4$ solution and dried at 70 °C.

Figure S21. EDX spectrum of the CC@*a*-MVO/MVN cathode at full charge.

Figure S22. SEM images of the Zn anode (a) before and (b) after 2000 cycles.

Figure S23. XRD pattern of the Zn anode after 2000 cycles.

Table S1. Comparison of the electrochemical performances of other reported V-based cathode materials for AZIBs.
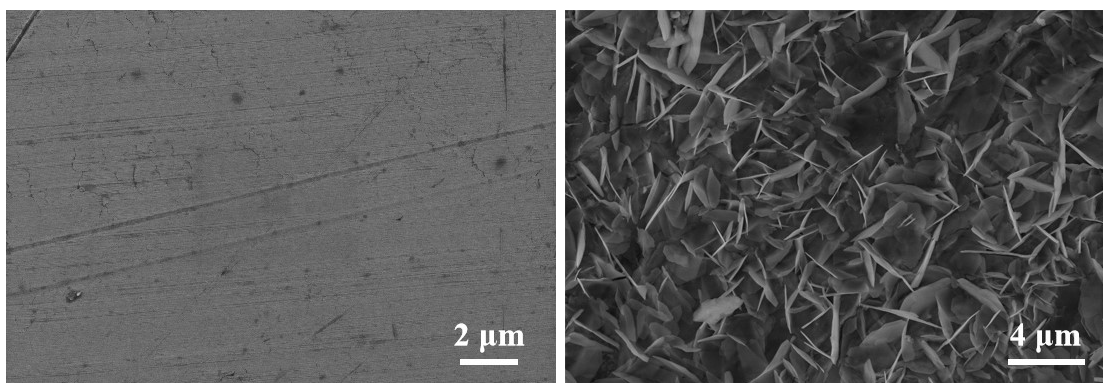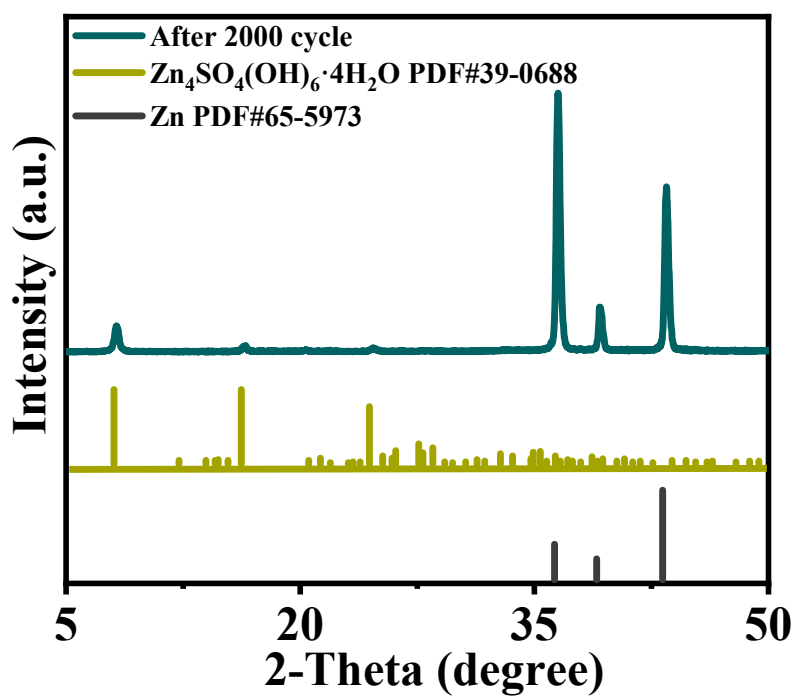
Cathode	Electrolyte	Specific Capacity	Cycling Performance	Ref.
CC@a−MVO/MVN	3 M $ZnSO_4$	265 mAh g^{-1} at 0.125 A g^{-1} 167.5 mAh g^{-1} at 2.5 A g^{-1}	94% retained after 2000 cycles at 1.5 A g^{-1}	This work
$K_2V_2O_3$	2 M $ZnSO_4$	139 mAh g^{-1} at 2 A g^{-1}	83% retained after 300 cycles at 6 A g^{-1}	16
$Zn_3V_2O_7(OH)_2 \cdot 2H_2O$	1 M $ZnSO_4$	54 mAh g^{-1} at 3 A g^{-1}	68% retained after 300 cycles at 0.2 A g^{-1}	17
Al−doped $VO_{1.52}(OH)_{0.77}$	1 M $ZnSO_4$	156 mAh g^{-1} at 0.015 A g^{-1}	≈78% retained after 50 cycles at 0.015 A g^{-1}	22
$VOPO_4 \cdot xH_2O$	13 M $ZnCl_2$+ 0.8 M H_3PO_4	170 mAh g^{-1} at 0.02 A g^{-1}	≈92% retained after 500 cycles at 2 A g^{-1}	23
VS_2	1M $ZnSO_4$	121.5 mAh g^{-1} at 1 A g^{-1}	98% retained after 200 cycles at 0.5 A g^{-1}	24
VS_2@N-C	3 M $Zn(CF_3SO_3)_2$	149 mAh g^{-1} at 1 A g^{-1}	97% retained after 1000 cycles at 1 A g^{-1}	44
$Zn_2(OH)VO_4$	Fumed silica/$ZnSO_4$	160 mAh g^{-1} at 2 A g^{-1}	89% retained after 2000 cycles at 4 A g^{-1}	48
$Na_{1.1}V_3O_{7.9}$	1 M $Zn(CF_3SO_3)_2$	112 mAh g^{-1} at 0.5 A g^{-1}	92.5% retained after 500 cycles at 1 A g^{-1}	56
VSe_2	2 M $ZnSO_4$	79.5 mAh g^{-1} at 2 A g^{-1}	75.3% retained after 500 cycles at 0.5 A g^{-1}	57
LiV_3O_8	1 M $ZnSO_4$	29 mAh g^{-1} at 1.66 A g^{-1}	75% retained after 65 cycles at 0.133 A g^{-1}	58
$Na_2V_2(PO_4)_2F_3$	2 M $Zn(CF_3SO_3)_2$	33 mAh g^{-1} at 3 A g^{-1}	95% retained after 4000 cycles at 1 A g^{-1}	59
$Na_3V_2(PO_4)_3$	2 M $Zn(CF_3SO_3)_2$	82 mAh g^{-1} at 2 A g^{-1}	75% retained after 200 cycles at 0.5 A g^{-1}	S1
VS_2 nanosheets/rGO	3 M $Zn(CF_3SO_3)_2$	174 mAh g^{-1} at 0.125 A g^{-1}	93% retained after 1000 cycles at 5 A g^{-1}	S2
V_2O_x@V_2CT_x	1 M $ZnSO_4$	224 mAh g^{-1} at 0.1A g^{-1}	81.6% retained after 200 cycles at 1 A g^{-1}	S3
V^{4+}-V_2O_5	2 M $ZnSO_4$	188.7 mAh g^{-1} at 0.5 A g^{-1}	≈72% retained after 1000 cycles at 10 A g^{-1}	S4

NH$_4$V$_4$O$_{10}$	3 M Zn(CF$_3$SO$_3$)$_2$	126 mAh g^{-1} at 0.2 A g^{-1}	70.3% retained after 5000 cycles at 2 A g^{-1}	S5
(NH$_4$)$_2$V$_{10}$O$_{25}$· 8H$_2$O	2 M ZnSO$_4$	228.8 mAh g^{-1} at 0.1 A g^{-1}	94.2% retained after 1000 cycles at 0.5 A g^{-1}	S6
Zn$_2$V$_2$O$_7$	1 M ZnSO$_4$	248 mAh g^{-1} at 0.1 A g^{-1}	85% retained after 1000 cycles at 4 A g^{-1}	S7
HfO$_2$−coated Zn$_3$V$_2$O$_7$(OH)$_2$· 2H$_2$O	1 M ZnSO$_4$	215 mAh g^{-1} at 0.1 A g^{-1}	84% retained after 1000 cycles at 10 A g^{-1}	S8
Cu$_3$V$_2$O$_7$(OH)$_2$· 2H$_2$O	2.5 M Zn(CF$_3$SO$_3$)	216 mAh g^{-1} at 0.1 A g^{-1}	89.3% retained after 500 cycles at 0.5 A g^{-1}	S9
Na$_3$V$_2$(PO$_4$)$_3$	0.5 M Zn(CH$_3$COO)$_2$	97 mAh g^{-1} at 0.05 A g^{-1}	74% retained after 100 cycles at 0.05 A g^{-1}	S10

References

S1 P. Hu, T. Zhu, X. Wang, X. Zhou, X. Wei, X. Yao, W. Luo, C. Shi, K.A. Owusu, L. Zhou and L. Mai, *Nano Energy,* 2019, **58**, 492–498.

S2 T. Chen, X. Zhu, X. Chen, Q. Zhang, Y. Li, W. Peng, F. Zhang and X. Fan, *J. Power Sources,* 2020, **477**, 228652.

S3 R. Venkatkarthick, N. Rodthongkum, X. Zhang, S. Wang, P. Pattananuwat, Y. Zhao, R. Liu and J. Qin, *ACS Appl. Energy Mater.*, 2020, **3**, 4677–4689.

S4 F. Liu, Z. Chen, G. Fang, Z. Wang, Y. Cai, B. Tang, J. Zhou and S. Liang, *Nano-Micro Lett.,* 2019, **11**, 25.

S5 G. Yang, T. Wei and C. Wang, *ACS Appl. Mater. Interfaces,* 2018, **10**, 35079–35089.

S6 T. Wei, Q. Li, G. Yang and C. Wang, *J. Mater. Chem. A,* 2018, **6**, 20402–20410.

S7 B. Sambandam, V. Soundharrajan, S. Kim, M.H. Alfaruqi, J. Jo, S. Kim, V. Mathew, Y.-K. Sunc and J. Kim, *J. Mater. Chem. A,* 2018, **6**, 3850–3856.

S8 J. Guo, J. Ming, Y. Lei, W. Zhang, C. Xia, Y. Cui and H.N. Alshareef, *ACS Energy Lett.,* 2019, **4**, 2776–2781.

S9 L. Chen, Z. Yang, J. Wu, H. Chen and J. Meng, *Electrochim. Acta,* 2020, **330** 135347.

S10 G. Li, Z. Yang, Y. Jiang, C. Jin, W. Huang, X. Ding and Y. Huang, *Nano Energy,* 2016, **25**, 211–217.